



Investigation of design and effects of a morphing winglet by applying a shape-memory alloy material on a passenger aircraft

Bir yolcu uçağına şekil hafızalı alaşım malzemesi uygulanarak dönüşen kanatçık tasarımının ve etkilerinin araştırılması

Ahmet Kaplan¹ , Sedat Nezh Karaal² , Rafet Bodur³ , Hasan Bora⁴ , Gorkem Sakaci⁵ ,
Furkan Datli⁶ , Fahrettin Ozturk^{7,*} 

^{1,2,3,4,5,6,7} Turkish Aerospace Industries, 06980, Ankara, Türkiye

⁷ Ankara Yıldırım Beyazıt University, Department of Mechanical Engineering, 06760, Ankara, Türkiye

Abstract

Continuous research and development have focused on optimizing wing aerodynamics and reducing fuel consumption in air vehicles since their inception. Winglets, fixed curved structures at wingtips, gained significant attention during the oil crisis for their fuel-saving potential in the aviation industry. This study focuses on designing a morphing winglet using a shape memory alloy (SMA) for improved aerodynamic efficiency and fuel economy under various conditions. The XFLR5 software analyzes the wing's lift and drag ratios at different aircraft stages (take-off, cruise, landing) for different cant angles. Results indicate that a moving winglet enhances the lift/drag ratio and reduces induced drag. Cant angle and angle of attack (AOA) variations play key roles in increasing this ratio. Optimal values for different aircraft stages are determined and discussed alongside existing mechanisms for moving winglets. Experimental data validation from previous studies in the literature concludes the research.

Keywords: Morphing winglet, Variable cant angle, Shape memory alloy, morphing winglet mechanism

1 Introduction

Low fuel consumption is a highly critical issue in the aerospace industry. Therefore, civil aviation regulators are asking manufacturers to reduce the long-term cost of fuel consumption, reduce carbon dioxide CO_2 and nitrogen oxide NO_2 emissions and thus, increase the efficiency of aircraft consumption. In order to increase the efficiency, it is necessary to examine the aerodynamic structure of the aircraft. Aircrafts fly based on pressure differences on the wing surfaces. Therefore, speed and pressure of air passing under and over the wings differ to keep the aircraft in the air. Due to this pressure difference, lift-induced drag might occur. For example, a transport aircraft shows that the magnitude of the lift-induced drag can be 40 % of the total drag at cruise conditions and 80 - 90% of the total drag during take-off and climb conditions [1-5].

Öz

Sürekli araştırma ve geliştirme, başlangıcından bu yana hava araçlarında kanat aerodinamiğini optimize etmeye ve yakıt tüketimini azaltmaya odaklanmıştır. Kanat uçlarındaki sabit kavisli yapılar olan kanatçıklar, havacılık endüstrisindeki yakıt tasarrufu potansiyeli nedeniyle petrol krizi sırasında büyük ilgi görmüştür. Bu çalışma, çeşitli koşullar altında gelişmiş aerodinamik verimlilik ve yakıt ekonomisi için şekil hafızalı alaşım (SMA) kullanan bir geçiş kanatçığı tasarlamaya odaklanmaktadır. XFLR5 yazılımı, farklı eğim açıları için farklı uçak aşamalarında (kalkış, seyir, iniş) kanadın kaldırma ve sürüklenme oranlarını analiz eder. Sonuçlar, hareketli bir kanatçığın kaldırma/sürüklenme oranını artırdığını ve indüklenen sürüklemeyi azalttığını göstermektedir. Cant açısı ve hücum açısı (AOA) varyasyonları bu oranın artırılmasında anahtar rol oynamaktadır. Kanatçıkların hareket ettirilmesine yönelik mevcut mekanizmaların yanı sıra, farklı uçak aşamaları için en uygun değerler belirlenmekte ve tartışılmaktadır. Literatürdeki önceki çalışmalardan elde edilen deneysel verilerin doğrulanması araştırmayı sonuçlandırmaktadır.

Anahtar kelimeler: Dönüşen kanatçık, Değişken eğim açısı, Şekil hafızalı alaşım, Geçiş kanatçık mekanizması

One way to reduce lift-induced drag is to increase the wingspan. However, increasing the wingspan requires further strengthening of the wing structure. The increase in the wingspan also increases the moment affecting the wing. Aircraft manufacturers use a curved wing tip which they call "a winglet" in order to reduce lift-induced drag. Aircraft manufacturers have produced curved wing structures in different forms [6, 7]. Many studies have found that winglet addition to an aircraft can achieve a fuel burn reduction by about 4-6 %, reduce the take-off distance and increase the climb rate. Note that the fuel consumption of an aircraft should be minimized during the flight period. Studies on this subject suggest curved wingtip designs [3-5, 8].

In the winglet condition, vortices formed at the wing tips were reduced, and fuel savings were achieved. However, with this type of wing, there is also a decrease in the lifting

* Sorumlu yazar / Corresponding author, e-posta / e-mail: fahrettin71@gmail.com (F. Ozturk)

Geliş / Received: 11.12.2023 Kabul / Accepted: 27.12.2023 Yayınlanma / Published: 15.04.2024

doi: 10.28948/ngumuh.1396487

force, which is needed during take-off. By comparing these two situations, it could be adjusted in the most efficient positions with a morphing winglet. In Figure 1, the use of winglets on aircraft can reduce the impact of vortex separations, which occur when air moves from high to low pressure. This effect is demonstrated by comparing the vortex separations with and without winglets on the aircraft.

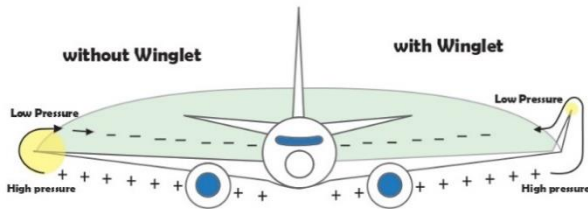


Figure 1. Vortex distribution for different wingtips

As the wing's lift deflects air, the overall lift vector is tilted backward. The aft component of the lift vector induces drag. Thus, induced drag is the rear component of the lift vector. By increasing the lift system's horizontal span or vertical height, the induced drag can be reduced (i.e. the length of the trailing edge holding the vortices can be increased). The lift force at the wing tips increases by widening the distribution of the vortices along the trailing edge through vanes. As a result, the induced drag is reduced. The induced drag reduction's main benefit depends on the wing's lift distribution in the direction of the wing span [6].

Figure 2 proves that the total drag of the wing with the winglet is less than the total drag of the wing without the winglet while operating above the crossing line or the line passing through the crossing point (the place where the two poles connect). In comparison, the overall drag of the wing without a winglet is lower than that of the wing with winglets when operating below the diagonal line. Therefore, winglets should not be used if you want to reduce overall drag. On the other hand, the employment of a winglet is aerodynamically justifiable if the wing is to function in ascending conditions (the light grey zone in Figure 2), as the wing creates less drag for a given lift. As a result, an aircraft may be more effective if its wing form can be modified according to its flight mission [9].

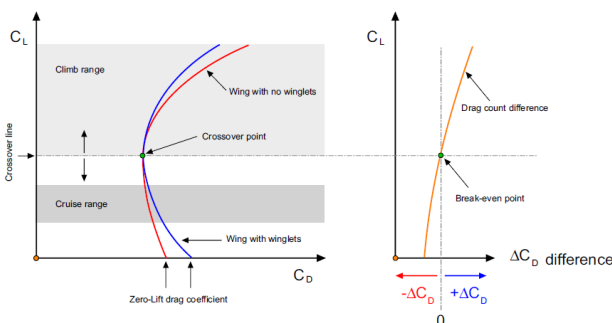


Figure 2. The drag polar of two hypothetical wings in an assumed flight condition [9]

During the 1970s and 1980s, researches conducted by NASA [10, 11] led to the development of vertical extensions that can be attached to wing tips to reduce aerodynamic drag without increasing the wing span. The first aircraft to adopt winglets were within the general aviation and business jet communities. In the mid-eighties, Boeing produced the 747-400 commercial jetliner, which used winglets to increase its range [12].

The SMAs are a class of metallic materials that have the ability to return to a predefined shape or size when subjected to certain stimuli, typically heat. They can undergo a reversible phase transformation from a low-temperature, deformed state to a high-temperature, stress-free state. When the material is heated, it reverts back to its original shape, and when it is cooled again, it retains that shape until the next heating cycle [13].

Crystal structure is an important factor that determines the physical and chemical properties of materials. Crystal structure affects the hardness, fracture toughness, thermal conductivity, electrical conductivity, optical properties and many other properties of materials. As described in Figure 3, these alloys are sensitive to heat changes and can also have two different crystal structures above or below critical conversion temperatures. Although they deform at low temperatures, they can return to their former state at high temperatures [14].

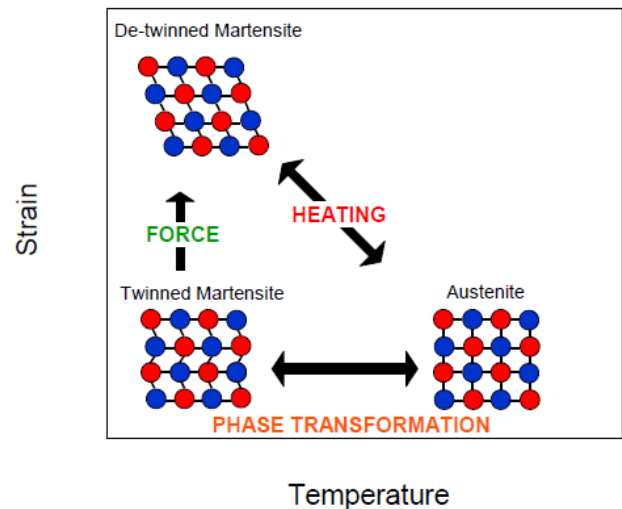


Figure 3. Temperature and load-induced phase transformations in the SMAs [13]

At high temperatures, nitinol assumes an interpenetrating simple cubic structure referred to as austenite (also known as the parent phase). At low temperatures, nitinol spontaneously transforms to a more complicated monoclinic crystal structure known as martensite (daughter phase). There are four transition temperatures associated to the austenite-to-martensite and martensite-to-austenite transformations [15].

Nitinol alloys exhibit two closely related and unique properties: the shape memory effect and superelasticity. Superelasticity is the ability for the metal to undergo large deformations and immediately return to its undeformed

shape upon removal of the external load. Nitinol can deform 10–30 times as much as ordinary metals and return to its original shape [16]. Crucial to nitinol properties are two key aspects of this phase transformation. First is that the transformation is "reversible", meaning that heating above the transformation temperature will revert the crystal structure to the simpler austenite phase. The second key point is that the transformation in both directions is instantaneous.

The Carnot cycle consists of four reversible processes: isothermal expansion, adiabatic expansion, isothermal compression, and adiabatic compression. The Carnot cycle is a theoretical construct and is not used in practice, but it is useful for exploring the efficiency limits. When the latter properties are important, the given design rules should be handled with care. In general, a SMA actuator can never have a greater efficiency than a Carnot cycle between heating and cooling temperature [17].

Table 2. Efficiency and energy density of actuators manufactured using the NiTi alloys based on different loading types [18]

Loading Type	Efficiency (%)	Absorbed Amount (J/kg)
(Carnot)	9.9	-
Tensile	1.3	446
Torsion	0.23	82
Bending	0.013	4.6

Note: Calculated using only elastic deformation quantities for comparison

The benefit of using wires as an active element is that the material is used to its fullest extent and that the least amount of the SMA is used to generate the appropriate amount of work. Table 1 provides an illustration of the benefits of using tension laden straight wires. In order to compare three load situations, the numbers in this table were derived using a pure elastic deformation, which is merely an approximate estimate. There are similar considerable solutions in this field; most examples in this domain are folding winglets for ground-based operations [19-22], reduction of induced drag when the aircraft is in the air at different cant angles [23-25], wing load alleviation mechanisms [26]. In other examples, the SMA has been used to reduce induced drag when the aircraft is in the air at different cant angles, but less work has been done for this purpose [27-29].

The temperature required to induce the shape-memory effect in shape-memory alloys is determined by their chemical composition. For nickel-titanium alloys, this temperature range is between -100 and +100 °C. It's important to note that there is a limit to the amount of strain that shape-memory alloys can withstand. If the material is deformed beyond this limit, full shape recovery cannot be achieved. The strain limit for nickel-titanium alloys is approximately 8.5%, which is high enough for many aerospace applications [30].

The variables in the wing must be determined to find the optimum position at different stages for a designed wing and winglet. Thus, the optimum position can be found by analyses by changing aerodynamic and characteristic properties of the wing. Some of the affecting wing

aerodynamics are AOA, sweep angle, cant angle and aspect ratio. These values vary according to different conditions and requirements for aircrafts. For this reason, parametric analysis, variables and constants should be determined.

The AOA is the angle between oncoming air or relative airstream and a chord line on the aircraft. Sometimes the reference line connects the leading and trailing edges at an average point on a wing. Most commercial jet aircraft use the fuselage centerline or longitudinal axis as the reference line [31].

As the nose of the wing turns up, the geometric AOA as well as lift increases. Drag goes also up, but not as quickly as lift. Therefore, increasing the geometric AOA until a certain point is efficient because of the increasing lift. This certain point is called critical or stall angle-of-attack. The lift coefficient decreases as the AOA decreases below the critical AOA. Conversely, as the AOA increases over the critical angle-of-attack, air begins to flow less smoothly across the airfoil's upper surface and begins to separate from it.

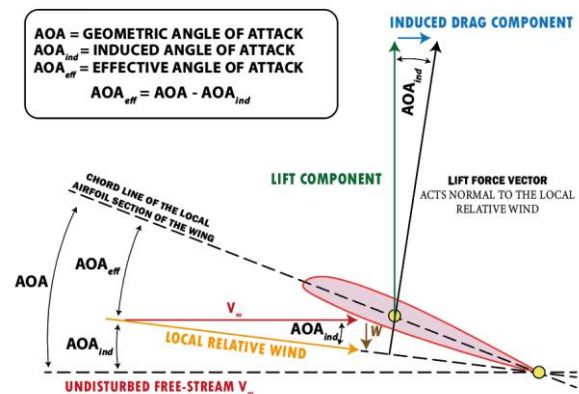


Figure 4. The AOA on an airfoil

The cant angle is an important parameter that should be considered in the design when aerodynamic factors are considered in the airfoil system. As seen in Figure 4, the cant angle is the angle of the winglet's normal line with the wing's normal line parallel to the surface. The cant angle determined as an independent variable in our analyses is shown in Figure 5. It is determined as the angle made by the wing tip with the horizontal.

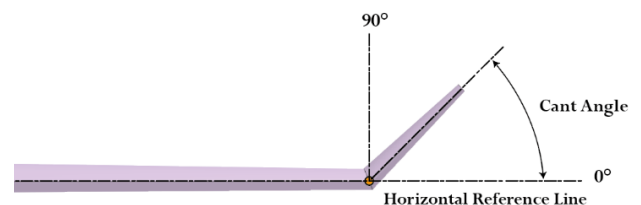


Figure 5. Cant angle relative to the horizontal reference line on the wing with winglet

Wing span is defined as the width of an aircraft wing as shown in Figure 6. It represents the longest distance from one

end of the wing to the other. This distance directly affects lift and drag of the wing. As the wing span increases, so does the lift of the wing, but also the drag. Wingspan is considered a decisive parameter in wing design. It is related to the size, weight, and placement of the wing and is one of the main design factors that affect the performance of aircraft.

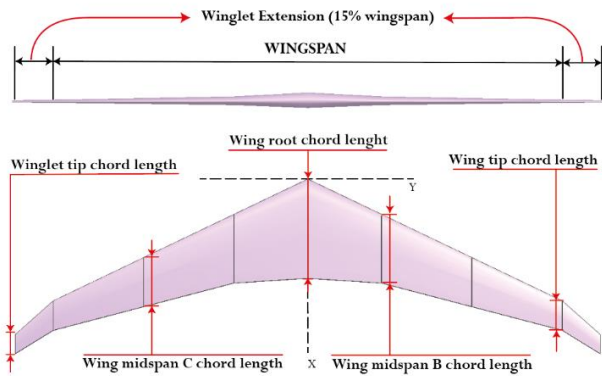


Figure 6. The front view of the wing with a winglet in the Figure on the top, the top view of the wing with a winglet, and the wing with winglet parameters in the Figure on the bottom

Sweep angle is the angular change of the wing from the root to the tip, which is the difference between the angle which the wing makes with the horizontal plane at the root and at the tip. This angle on the designed winglet is shown in Figure 7. This parameter affects the aerodynamic performance of the wing, especially the behavior of the boundary layer at the wingtip.

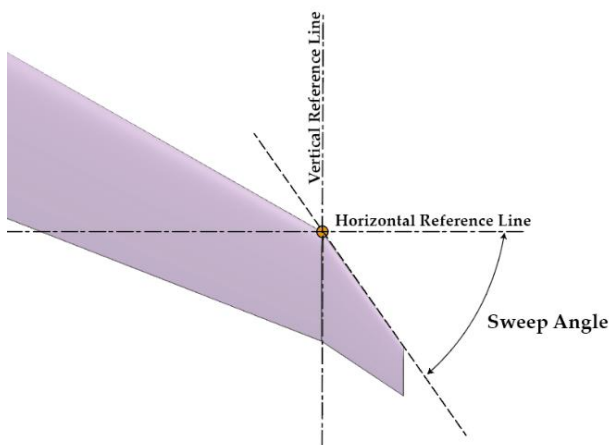


Figure 7. Winglet sweep angle according to the vertical and horizontal reference lines on the wing with winglet

As the speed of the aircraft increases, airflow passes over the wing more quickly and the wing generates more lift. However, at high speeds, the drag also increases, which increases the resistance of the wing. Therefore, the design of aircraft is optimized according to their speed, and the design of the winglet is also made in accordance with this speed.

The speed of the aircraft can be expressed by the Mach number. The Mach number is a parameter that expresses the speed of the aircraft in relation to the speed of reaching sound (the speed of sound). The wing design and the aerodynamic performance of the winglet are closely related to the Mach number of the aircraft.

Airfoil design is an important parameter in winglet design. The airfoil is defined as the cross section of the wing. It greatly affects the aerodynamic performance of the wing. The airfoil design is determined to optimize buoyancy, resistance, and strength characteristics of the winglet. The airfoil design, working together with the shape, size and sweep angle of the wing, determines aerodynamic characteristics of the wing. The aerodynamic efficiency of the wing and the design of the airfoil is typically studied carefully to make sure that the airfoil design is done correctly and is compatible with other factors in the design of the winglet. Since a passenger aircraft is examined in this study, the Boeing-737 airfoil is applied.

2 Method and analysis

In this study, a mechanism capable of different cant angles was targeted. According to this purpose, the cant angle should be set in the horizontal position in the same position as the base wing or the vertical position (including intermediate cant angles). Moreover, the winglet can be positioned according to the best lift-induced drag reduction for different flight conditions (take-off, climb, cruise, landing). When the aircraft is on the ground, the wingspan can be reduced to fit more easily into gangways and hangars. In different weather conditions, the winglet can be adjusted to the position that will apply the least moment to the aircraft with the winglet feedback system in side winds.

First, speeds of a commercial aircraft under optimum take-off and cruise conditions were taken into account. Mach number equivalents of these values were determined as 0.3 for take-off and 0.84 for cruise [32]. Furthermore, depending on results of numerical studies, winglet angles at which the best aerodynamic performance is obtained according to the flight phases are proposed. Then, based on these optimizations, a mechanism using the SMA is suggested to move the winglet.

One of the objectives of this research is to compare drag and lift forces of the aircraft at take-off and cruise stages using the different AOA values. In this way, it is desired to be able to comment on the induced drag change. Figure 8 shows the layout of these airfoils on the Boeing 737 wing. While designing the wing, the wing parameters of the Boeing 737 aircraft were taken and scaled [33]. Winglet span, according to the information obtained from the sources, is recommended to take 10-20% of the wing span determined for the baseline wing [1,34]. In this study, the wingspan was determined as 15%. Additionally, a sweep angle of 60° was selected, as shown in Figure 7, which yielded the best efficiency according to the research [9]. Since the aircraft will be moving at low speeds during take-off, analysis results at Ma= 0.3 and higher AOA values are relevant for the state of the aircraft during take-off. For the aircraft during the

cruise, the analysis is performed for $Ma=0.84$ and lower AOA values.

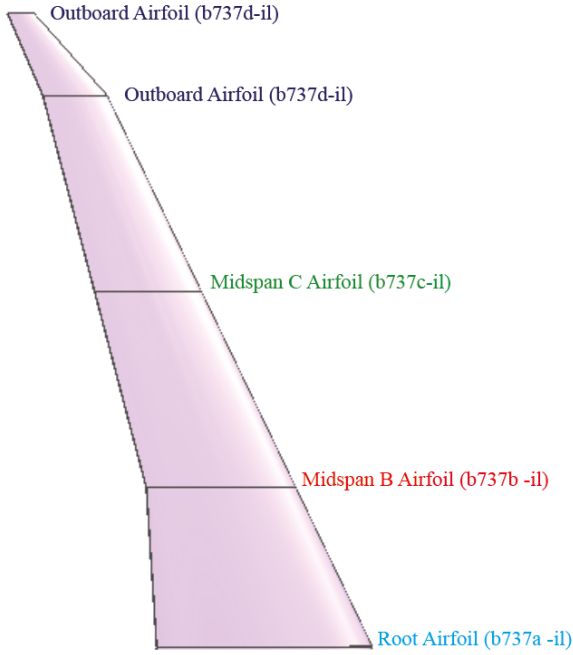


Figure 8. Boeing 737 airfoil layout on the wing

All required data for the analysis are summarized and given in [Table 2](#) and [3](#).

Table 2. The wing parameters for the analysis

Design Variables	Values
Winglet cant angle	0°, 15°, 45°, 80°
Angle-of-attack at $Ma = 0.3$	0°-20° (spaced at intervals of 2)
Angle-of-attack at $Ma = 0.84$	0°-10° (spaced at intervals of 2)

Table 3. The wing parameter constants for the analysis

Design Constants	Values
Wing airfoil geometries	Boeing 737
Winglet sweep angle	60°
Wingspan	Base wing + 15 %

In this study, analyses were performed using the XFLR5 software. Neumann and Dirichlet can be selected for the far-field boundary condition in the analysis. Thus, there are no significant gradients normal to surface boundaries. The wing is modeled as a no-slip wall, i.e. a continuous wall for turbulent values. There are four different analysis methods for XFLR5; LLT (wing only), Horseshoe vortex (VLM1) (No sideslip), Ring vortex (VLM2), and 3-D Panels methods. In this study, analyses are performed using the 3-D Panels method. Documentation for the software states that viscous effects might not be captured properly especially for the 3D panel method (leading to 20% error in lift coefficient estimates). It provides the opportunity to observe breaks in the transition from wing to fin by obtaining the pressure graph. When wing and winglet were modeled in accordance with these parameters, the first airfoil analysis was

performed. These analyzes were performed with different Reynolds numbers that were increased regularly because the XFLR5 program determines trends of the aircraft in different weather conditions and at different speeds after the integration of the airfoil into the wing according to the data obtained from this airfoil analysis. For this reason, we introduced the program by increasing the iterations by considering all conditions while performing the airfoil analysis. Note that it is desired to obtain a result by converging the Reynolds number to one value at different AOA values at different velocities. After this 2D airfoil analysis, we created a 3D wing structure and interpreted these results by obtaining the lift force, drag force, induced drag and Lift/Drag ratio for the wing using the 3-D Panels method.

Lift (L) and drag (D) forces are obtained by integrating pressures applied to the wing surface and wall shear stresses. Lift coefficient C_L and drag coefficient C_D are obtained as follows,

$$C_L = \frac{L}{0.5 \times \rho \times V_\infty^2 \times S_{ref}} \quad (1)$$

and

$$C_D = \frac{D}{0.5 \times \rho \times V_\infty^2 \times S_{ref}} \quad (2)$$

where ρ is the air density, V_∞ is the free-stream velocity and S_{ref} is the wing reference area. It is the wing area in the top view when specifying the S_{ref} for the lift. S_{ref} for drag is the wing area in the front view. By the flight principle, the drag force should be reduced while trying to increase the lift force. An aerodynamic efficiency parameter (C_L/C_D) is obtained based on this situation. The higher this value, the higher the efficiency will be.

3 Mechanism design

The design was developed based on an extensive review of existing research and studies on winglet mechanisms developed with and without the SMA. The main objective is to propose a new winglet movement mechanism using the SMA that meets desired criteria. The aim of this study is to determine advantages and limitations of the SMA-based mechanisms over their non-SMA counterparts by examining the current situation in winglet design. Results might contribute to the development of an optimized SMA-based winglet mechanism with improved performance.

The primary objective of this study is to achieve the desired winglet angle by converting linear movement into rotational movement through heating SMAs within a range of motion between 0° and 90°. Furthermore, the mechanism should incorporate a locking system to ensure the winglet angle remains fixed at the desired position.

In the design of the winglet movement mechanism, emphasis is placed on minimizing friction losses to optimize the movement power of the SMAs. The mechanism is designed with simplicity in mind, utilizing a limited number of materials and straightforward elements. This approach

facilitates easy maintenance and assembly processes. Additionally, careful consideration is given to the size and strength of the mechanism to ensure suitability for the wingtip application.

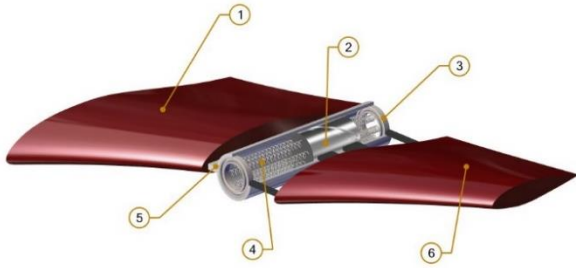


Figure 9. BOM ID of mechanism components

Table 4. Name, quantity, and material properties according to the BOM ID

BOM ID	Name	Quantity	Material
1	Base wing	1	Composite
2	Female slot cylinder	1	Aluminum alloy
3	Roller	1x2	Chrome steel
4	SMA spring	6x2	Shape memory alloy
5	Mechanism bearing-male slot	1	Aluminum alloy
6	Winglet	1	Composite

Table 4 shows the bill of material of the parts of the mechanism. The working logic of the mechanism (Figure 9) is described as follows:

The working principle of the mechanism is the conversion of linear motion into rotational motion.

Heating the SMA springs with the help of electric current creates linear motion. This movement causes the female-slot cylinder in the mechanism to make a rotational movement. This movement is transferred directly to the winglet and allows the angle of the winglet to be changed.

When the desired angle is reached with the help of the encoder, it is assumed that the locking mechanism in the system activates and ensures the fixation of the mechanism at this angle (Figure 10).

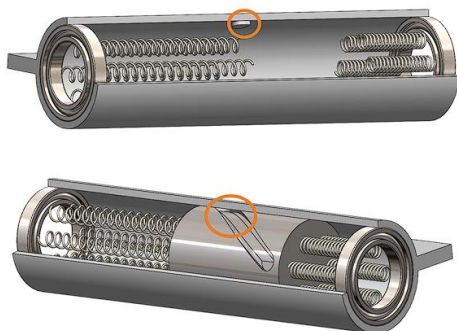


Figure 10. Top: Male slot. Bottom: Connection with female slot

The power to be obtained with the amount of the SMA to be used in the mechanism depends on the weight of the winglet, the forces it is exposed to during flight, the losses of the mechanism due to friction, the difficulty of the SMAs on opposite sides against the movement and the difficulty of the locking mechanism used.

Depending on the power requirement, the number of mechanisms to be used and their dimensions may vary. With these changes, compact and synchronous operation of the mechanism is important. Insulation techniques will be used to keep the SMA springs at the desired temperature. A control mechanism is also required to provide remote control of the mechanism.

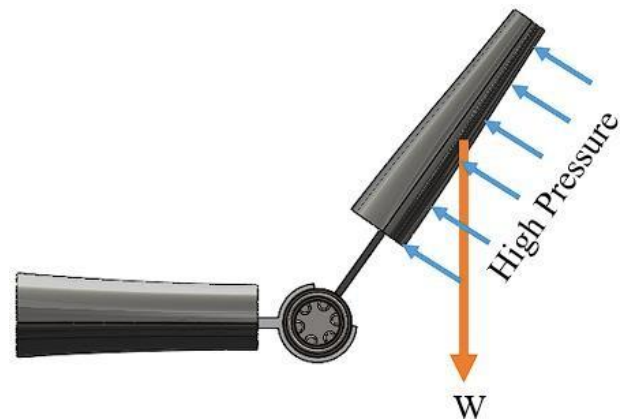


Figure 11. Weight and high-pressure vectors acting on the winglet

Figure 11 displays the forces acting on the winglet. Due to the difficulty of by high pressure due to the airflow during the change of angle of the winglet, the weight of the winglet alone is insufficient to move in reverse. The reason why the SMA springs are used on both sides of the mechanism is that it provides force in addition to weight to overcome this high pressure.

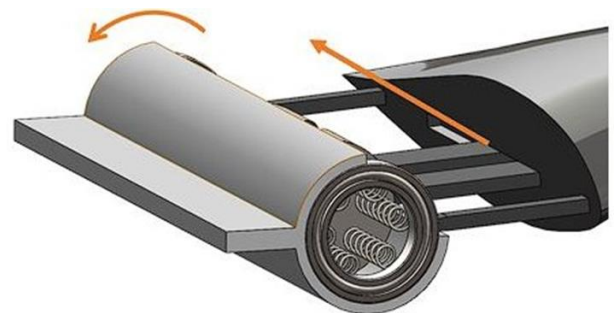


Figure 12. Slot on the winglet not affected by the linear movement of the cylinder as it rotates

While the cylinder in the mechanism converts the linear movement it receives from the SMA springs to rotational movement, its horizontal movement should not be transferred to the winglets. It is desirable to change the angle of the winglet only by vertical movement. Therefore, as shown in Figure 12, there is an open slot in the middle that

connects the winglet to the mechanism, thus, absorbing the horizontal movement.

Advantages:

Mechanical simplicity: The design of the mechanism is simple and does not require a large number of components. This reduces the complexity of the system and makes it easier to manufacture and maintain.

Lightness: The mechanism is lightweight, which is important because any additional weight at the wing tips can create extra momentum and reduce fuel efficiency. The use of small springs and a small number of elements contributes to the lightness of the mechanism.

Cost: The use of a movable blade model reduces the cost of the mechanism. This is because the movable blade model is less expensive to manufacture than a fixed blade model. Additionally, the movable blade model requires less maintenance, which further reduces the overall cost of the mechanism.

Disadvantages:

Power Requirements: The SMA materials require significant amounts of electrical power to heat and activate their shape memory effect. This could result in increased power consumption, especially if the multiple SMA elements are used in the mechanism.

Control Complexity: The SMA-based mechanisms often require precise control systems to achieve the desired movement and angle. Developing and implementing a reliable control algorithm for the mechanism may be challenging, especially if it involves multiple SMA elements and interaction with other control systems in the aircraft.

4 Results and discussion

Results of analyses of the aerodynamic performance of the wing with winglets at different cant angles are presented. They correspond to the Mach number equal to 0.84, which is the cruise speed of a typical civil aircraft. In addition, conclusions were made regarding the state of the aircraft and winglet at different cant angles with respect to the variation of the AOA from 0° to 10° and the subsonic cruise level changes at medium and long distances. As seen in Figure 14, when the cant angle increases, $C_{L,max}$ decreases due to the decrease in the pressure difference. In contrast, when the cant angle decreases, $C_{L,max}$ increases since the change in the pressure difference due to the winglet also affects the drag, as shown in Figure 13. However, in this case, the reduction in pressure difference has a positive effect on the drag and intensity of the wingtip vortices.

The wing aerodynamic performance will be compared for C_D values at the same C_L value for different positions in the air. Since less C_L is required when the aircraft is on cruise, the average change in C_D between $C_L = 0.1$ and $C_L = 0.2$ was analyzed. Since higher C_L is required for cruise level changes, C_L was taken as 0.35. Results are summarized in Table 5 and 6 for the cruising state ($0.1 < C_L < 0.2$). The highest drag reduction value was observed between 0° and 45°. For cruising level change ($C_L = 0.35$), the optimum result was obtained at cant angle values of 15°. However, 45°

cant angle is also acceptable to create less drag at the same C_L value.

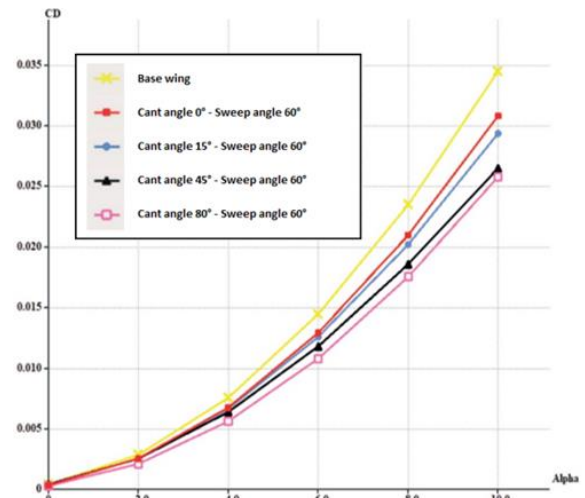


Figure 13. Drag coefficient versus the AOA at the Mach number of 0.84, sweep angle of 60° and different values of cant angle

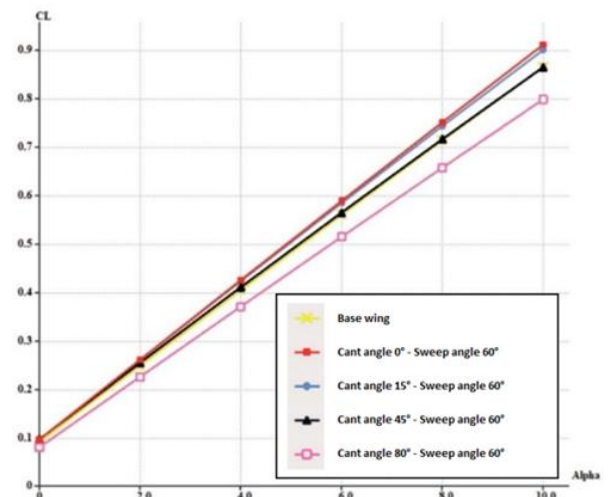


Figure 14. Lift coefficient versus the AOA at the Mach number of 0.84, sweep angle of 60° and different values of cant angle.

Table 5. C_D and drag reduction percentage for a target C_L between 0.1 to 0.2 at the Mach number of 0.84

Winglet cant angle	C_D	3D Wing Drag reduction (%)
0°	0.00218	10.1
15°	0.00216	11.2
45°	0.00252	-3.2
80°	0.00249	-2.0

Table 6. C_D and drag reduction percentage for a target C_L equal to 0.35 at the Mach number of 0.84

Winglet cant angle	C_D	3D Wing Drag reduction (%)
0°	0.00481	17.1
15°	0.00472	18.6
45°	0.00488	15.9
80°	0.00512	11.7

Secondly, the aerodynamic performance analysis for civil aircrafts at constant sweep angles and different cant angles for take-off and landing cases (for $Ma = 0.3$) is presented. In addition, analyses have also been carried out considering the change in the AOA. The AOA value can be up to 20° at take-off, and the change of different parameters (induced drag, lift) was observed for the AOAs up to 20° . The points discussed in this section are similar to those in earlier, since $Ma = 0.3$, compressibility effects and wave drag cannot be mentioned in this stage. Thus, increasing the cant angle leads to a noticeable reduction in C_L . As for the pressure difference, larger cant angles result in decreased pressure towards the wing's tip, contributing to the reduction in C_L . A higher pressure difference during take-off benefits lift force. Comparing configurations, the winglet setup with 0° cant angle exhibits the smallest C_D at low speeds, explaining the use of winglets. Figure 15 demonstrates that increasing the cant angle proportionally increases C_D , with the most significant drag reduction occurring at cant angles between 45° and 15° is mainly because it is the biggest cant angle increase. In Figure 16, at a sweep angle of 60° , C_L remains stable up to 2° AOA, peaking at 20° AOA for the winglet configuration with 0° cant angle. However, the winglet with 80° cant angle minimizes C_D at high AOA, potentially affecting the lift force during take-off (at low Mach numbers and high AOA values).

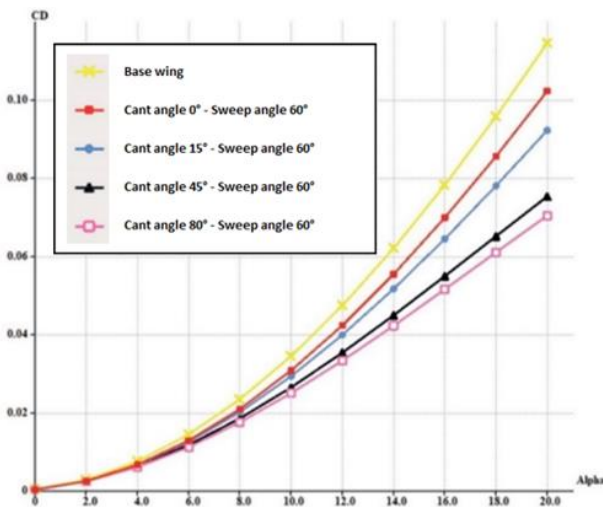


Figure 15. Drag coefficient versus the AOA at the Mach number of 0.3, sweep angle of 60° and different values of cant angle

For the same C_L value for the wing aerodynamic performance at take-off, C_D values were compared. $C_L = 0.6$ is taken because higher C_L is required during the take-off of the aircraft.

According to the results in Table 7, the highest drag reduction for the take-off phase ($C_L = 0.6$) is the configuration where the cant angle is 80° . As it is known, as the cant angle value increases, the C_D value increases in parallel with it and the drag reduction value decreases. In addition, with these results, one of the significant reasons why winglet is used again becomes apparent.

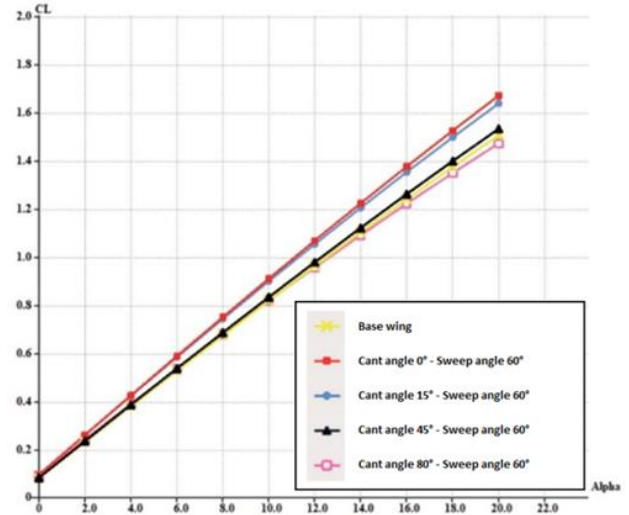


Figure 16. Lift coefficient versus the AOA at the Mach number of 0.3, sweep angle of 60° , and different values of cant angle

Table 7. C_D and drag reduction percentage for a target C_L equal to 0.6 at the Mach number of 0.3

Winglet cant angle	C_D	3D Wing Drag reduction (%)
0°	0.0134	20.238
15°	0.0135	19.643
45°	0.01385	17.56
80°	0.0141	16.07

The analyses performed in this study reveal that no single winglet configuration provides the best drag reduction for a flight phase. Therefore, positioning the winglet cant angle to optimize the aerodynamic performance in different flight phases is the main topic of the conclusion. The proposed winglet positioning is shown in Figure 17 for each flight phase. Suggestions for the optimum configuration for flight phases are summarized as follows:

When the aircraft is on the wheel, it is advised that the cant angle should be 80° to reduce the wingspan and make gate transitions easier.

As seen from the analyses, the 15° cant angle provides more drag reduction for the take-off phase of the aircraft. However, by using a 45° cant angle, more lift-slope can be obtained by sacrificing some drag reduction. This can be used in conditions where it is desired to provide extra lift for the take-off phase of the aircraft. This selection can be decided by considering the take-off distance according to the take-off weight of the aircraft, weather conditions and runway conditions.

The configuration with the highest drag reduction obtained from the analysis cant angle of 15° is preferred since there is no additional lift-slope requirement in the cruise phase of the aircraft a (high Mach number). In addition, although high drag reduction is also achieved at 0° cant angle, it is not suggested to use 0° cant angle as it will cause more root bending moment in the wing at this position. It is proposed that the cant angle should be 45° while changing the cruising altitude. The main reason is to obtain more drag reduction while obtaining more lift slope. A cant

angle of 15° is also acceptable in cases where extra lift-slope is required.

According to the analysis results in the landing phase, a cant angle of 45° is suggested, while an 80° winglet cant angle is not recommended. The reason for this is that it reduces C_{Lmax} .

It is advisable to use an 80° cant angle after landing and hangar entry situations. In this way, the wingspan is reduced to the minimum value, providing gate transitions convenience.

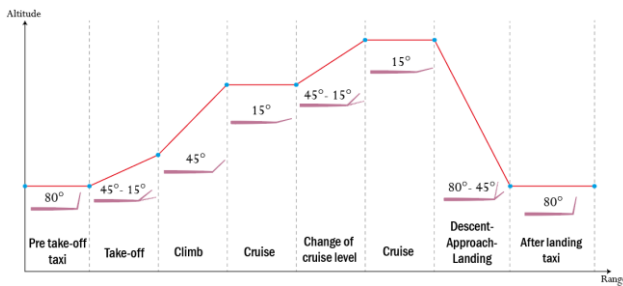


Figure 17. Winglet cant angle configuration during different flight phases

5 Conclusion

This study explores different tilt angle values to reduce optimal drag during various flight stages, using a wing designed to create guides for in-flight transition ailerons. Considering the different AOA values, high and low Mach numbers ($Ma = 0.84$ and $Ma = 0.3$) and the 60° sweep angle, the optimal inclination angle for take-off, climbing, cruising, and landing conditions was determined. As a result of the analyses, it is suggested that the aircraft should have a winglet angle of, 45° - 15° at the time of takeoff, 45° at the time of ascent, 15° while cruising, 45° - 15° during cruise level change and 80° - 45° at the time of landing. At the advanced stages of this study, CFD analysis can be performed, and more accurate data can be obtained. With physical tests (e.g. wind tunnel tests) The cant angle can be determined by comparing the analysis results. For the concept mechanism, the goal is to design an original winglet mechanism that converts linear motion into rotational motion using the tendency of the SMA springs to revert to their former state in a heat-sensitive manner, and a locking system to maintain the cant angle. The optimized design aims to minimize friction losses and provide simplicity and convenience, contributing to the improved SMA-based winglet mechanism. The power requirements of the mechanism can be determined according to the weight that it will lift, and the number of SMAs or the size of the mechanism can be changed.

Conflict of interest

The authors declare that there is no conflict of interest

Similarity rate (iThenticate): 15%

References

- [1] E. Torenbeek, *Advanced aircraft design: conceptual design, analysis and optimization of subsonic civil airplanes*. John Wiley & Sons, 2013.
- [2] J. E. Guerrero, D. Maestro and A. Bottaro, Biomimetic spiroid winglets for lift and drag control. *Comptes Rendus Mécanique*, 340, 1–2, 67–80, Jan. 2012. <https://doi.org/10.1016/J.CRME.2011.11.007>.
- [3] I. Kroo, *Nonplanar wing concepts for increased aircraft efficiency*. VKI lecture series on innovative configurations and advanced concepts for future civil aircraft, Stanford University, USA, 2005.
- [4] I. Kroo, *Drag Due to Lift: Concepts for prediction and reduction*, *Annual Review of Fluid Mechanics*. Palo Alto, 33, 1, 587–617, 2001. <https://doi.org/10.1146/annurev.fluid.33.1.587>.
- [5] Air Force Studies Board, and National Research Council, *Assessment of wingtip modifications to increase the fuel efficiency of air force aircraft*. National Academies Press, Washington, DC, 2007.
- [6] R. Faye, R Laprete and M. Winter, *Blended Winglets for Improved Airplane Performance*, *Aero*, Boeing, (17), January 2002.
- [7] B. S. de Mattos, A. P. Macedo and D. H. da Silva Filho, *Considerations about winglet design*. 21st AIAA Applied Aerodynamics Conference, 2003. <https://doi.org/10.2514/6.2003-3502>.
- [8] R. T. Whitcomb, *A design approach and selected wind tunnel results at high subsonic speeds for wing-tip mounted winglets*, NASA Langley Research Center Hampton, Washington, NASA Technical Note TN D-8260, July 1976.
- [9] J. E. Guerrero, M. Sanguineti and K. Wittkowski, *Variable cant angle winglets for improvement of aircraft flight performance*. *Meccanica*, 55, 10, 1917–1947, 2020. <https://doi.org/10.1007/S11012-020-01230-1>.
- [10] D. Hartl, B. Volk, D. C. Lagoudas, F. Calkins and J. Mabe, *Thermomechanical Characterization and Modeling of Ni60Ti40 SMA for Actuated Chevrons*. American Society of Mechanical Engineers, Aerospace Division (Publication) AD, 281–290, 2007. <https://doi.org/10.1115/IMECE2006-15029>.
- [11] J. Chambers, *Concept to reality: Contributions of the Langley Research Center to US Civil Aircraft of the 1990s*, 2003.
- [12] NASA, *NASA Contribution: Winglets*, 2015. <http://www.nasa.gov/aero/nasa-contribution-winglets.html>, Accessed: 15 November 2022.
- [13] E. Acar, *Precipitation, orientation and composition effects on the shape memory properties of high strength NiTiHfPd alloys*, Thesis, University of Kentucky, UK, 2014.
- [14] K. Otsuka and T. Kakeshita, *Science and Technology of Shape-Memory Alloys: New Developments*. *MRS Bull*, 27, 2, 91–100, 2002. <https://doi.org/10.1557/MRS2002.43>.
- [15] K. Otsuka and X. Ren, *Physical Metallurgy of Ti-Ni-based Shape Memory Alloys*. *Prog Mater Sci*, 50, 5, 511–678, 2005. <https://doi.org/10.1016/j.pmatsci.2004.10.001>.
- [16] T.R. Meling, *The effect of temperature on the elastic responses to longitudinal torsion of rectangular nickel*

- titanium archwires. *The Angle Orthodontist*, 68(4), 357-368, 1998. [https://doi.org/10.1043/0003-3219\(1998\)068<0357:TEOTOT>2.3.CO;2](https://doi.org/10.1043/0003-3219(1998)068<0357:TEOTOT>2.3.CO;2).
- [17] Y. A. Cengel and M. A. Boles, *Thermodynamics: An Engineering Approach*, 8th Edition, Chapter 1 Introduction And Basic Concepts, 2015.
- [18] D. Reynaerts and H. Van Brussel, Design aspects of shape memory actuators. *Mechatronics*, 8, 6, 635–656, 1998. [https://doi.org/10.1016/S0957-4158\(98\)00023-3](https://doi.org/10.1016/S0957-4158(98)00023-3).
- [19] J. B. Allen, Articulating winglets, U.S. Patent, US5988563A, 23 November 1999.
- [20] J. R. Veile, Wing fold push-pin locking assembly, U.S. Patent, US9469392B2, 19 April 1994.
- [21] R. M. Bray, Winglet, U.S. Patent, US7988099B2, 02 August 2011.
- [22] Boeing Commercial, Video: Boeing 777x folding wingtip. <https://www.boeing.com/777x/reveal/video-777x-FoldingWingtip/>, Accessed December 2022
- [23] B. Barriety, Wing load alleviation apparatus and method, U.S. Patent, US6827314B2, 07 December 2004.
- [24] P. Bourdin, A. Gatto and M. I. Friswell, Aircraft Control via Variable Cant-Angle Winglets, 45, 2, 414–423, 2012. <https://doi.org/10.2514/1.27720>.
- [25] P. Panagiotou, M. Efthymiadis, D. Mitridis and K. Yakinthos, “A CFD-aided investigation of the morphing winglet concept for the performance optimization of fixed-wing MALE UAVS,” *Aerospace Research Central*, 42, 2018. <https://doi.org/10.2514/6.2018-4220>.
- [26] P. Dees and M. Sankrithi, Wing load alleviation apparatus and method, U.S. Patent, US20070114327A1, 24 May 2007.
- [27] A. M. Pankonien, *Smart Material Wing Morphing for Unmanned Aerial Vehicles*. Thesis, University Of Michigan Library, USA, 2015.
- [28] P. Marks, ‘Morphing’ winglets to boost aircraft efficiency, *New Scientist*, 201, 2692, 22–23, 21 January 2009. [https://doi.org/10.1016/S0262-4079\(09\)60208-6](https://doi.org/10.1016/S0262-4079(09)60208-6).
- [29] NASA, NASA Tests New Alloy to Fold Wings in Flight. <https://www.nasa.gov/aeronautics/nasa-tests-new-alloy-to-fold-wings-in-flight/>, Accessed: 25 December 2022.
- [30] A.P. Mouritz, Titanium alloys for aerospace structures and engines, *Introduction to Aerospace Materials*, Woodhead Publishing Limited, Sawston, U.K., pp. 202–223, 2012. <https://doi.org/10.1533/9780857095152.202>.
- [31] M. Kumar, S. Bal and B. Girish, Proceedings of First Joint International Conference on Advances in Mechanical and Aerospace Engineering, pp. 239, Alliance University, Bengaluru, India, December 2023.
- [32] E. S. Rutowski, Energy Approach to the General Aircraft Performance Problem, *Aerospace Research Central*, 21, 3, 187–195, 2012. <https://doi.org/10.2514/8.2956>.
- [33] Boeing, 737 Airplane Characteristics for Airport Planing. <https://www.slideshare.net/RenzoJoseJuradoRolon/737-66864457/>, Accessed: 06 March 2024.
- [34] A. Thomas, W. Saric, A. Braslow and D. Bushnell, *Aircraft Drag Prediction and Reduction*. Defense Technical Information Center, France, Technical Report AGARD-R-723, 01 Jul 1985.

